

# Interhemispheric effects on ion upflow and neutral upwelling

Marc Lessard, Alec Damsell and Brent Sadler, University of New Hampshire

## Introduction

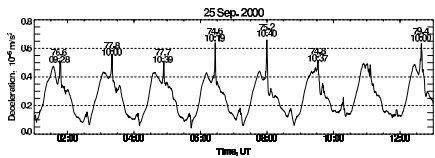
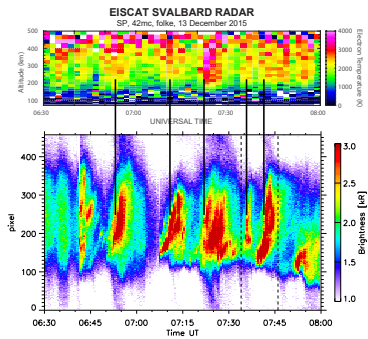


Figure 1. Accelerometer observations from the CHAMP satellite. This plot shows 12 hours of data, spanning a total of 8 orbits. The large-scale variations are the most obvious feature, with drag in the northern hemisphere being greater than in the southern hemisphere. This study, however, focuses on the narrow spikes that are associated with passes through the cusp region. The southern spikes are clearly much less significant than in the north.

## ?????

- Olson, D. [2012] used FAST and CHAMP satellite data to show a clear correlation between neutral upwelling and ion outflow.
- Cohen et al. [2015] show that increased density inhibits the strength of the ambipolar field and reduces upflow speeds. However, upflow fluxes are still enhanced at higher densities because more ions are present to be influenced by the field.
- Kervalishvili et al. [2018] show evidence for altitude-dependent neutral density perturbations based on CHAMP/GRACE comparisons and conclude that relative density perturbations at 500 km altitude are greater than at 400 km, especially in a dark ionosphere.

## PMAF effect



## Ionospheric variability

Figure 4. IRI predictions of density profiles for Longyearbyen for 4 different cases, to show the expected variability at that location (i.e., northern cusp). The light blue trace shows the profile for a dark ionosphere (Dec 21) during solar minimum; the dark blue trace also shows the profile for a dark ionosphere, but during solar maximum. The yellow trace shows the density for a sunlit ionosphere (Jun 21) during solar minimum; the orange trace also shows the profile for a sunlit ionosphere, but during solar maximum.

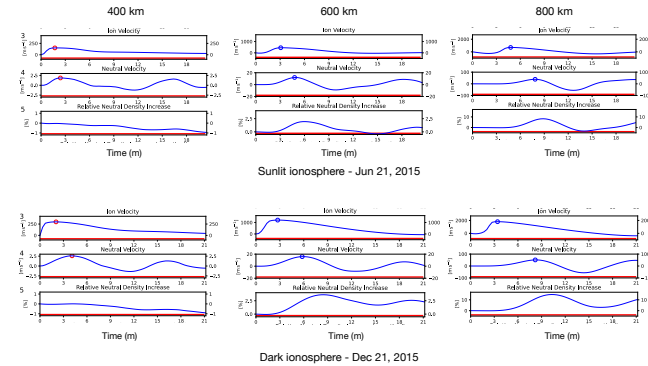
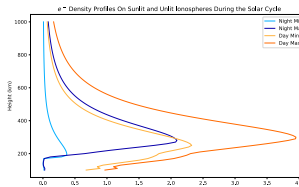
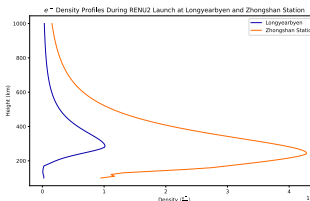


Figure 5. Model predictions of ion flow velocities, neutral particle velocities and relative neutral density variability. The top three panels show quantities during a sunlit ionosphere at Longyearbyen (typical cusp location), at altitudes of 400, 600 and 800 km. The bottom three panels show these quantities during a dark ionosphere, at the same location.

Parameters:		400 km	600 km	800 km
Ion velocity, m/s	Light	150	450	700
	Dark	300	1200	1800
Neutral velocity, m/s	Light	2.0	12	39
	Dark	2.6	1.6	51
Relative neutral density increase, %	Light	—	2.0	8.2
	Dark	—	3.6	14.9

Figure 3. Density profiles during the RENU2 launch. The blue trace shows IRI predictions; the green trace shows EISCAT observations at 7:35 UT, "in between" auroral arcs, which is similar to the IRI results except at a somewhat lower altitude. The orange trace shows IRI predictions for Zhongshan Station in Antarctica, nominally conjugate to Longyearbyen.



## Interhemisphere results

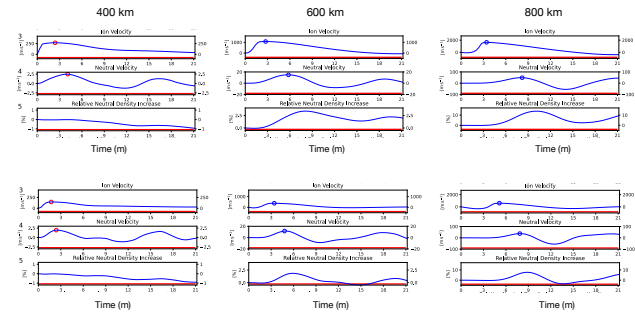


Figure 6. Model predictions of ion flow velocities, neutral particle velocities and relative neutral density variability, with the same format as in the previous figure. This provides an example of simultaneous interhemispheric predictions, with Longyearbyen in the northern hemisphere and Zhongshan Station (Antarctica). Density profiles for these model runs are shown in Figure 3.

Parameters:		400 km	600 km	800 km
Ion velocity, m/s	ZGN (light)	144	379	600
	LYR (dark)	268	1080	1650
Neutral velocity, m/s	ZGN (light)	2.0	12	37
	LYR (dark)	2.5	1.5	49
Relative neutral density increase, %	ZGN (light)	—	2.0	7.7
	LYR (dark)	—	3.4	14

## References

Cohen, I. J., et al. Ion upflow dependence on ionospheric density and solar photoionization, *J. Geophys. Res. Space Physics*, 120, 10,039–10,052, doi:10.1002/2015.JA021523.

Olson, D., *Neutral Gas and Plasma Interactions in the Polar Cusp*, David Olson, PhD Thesis, UMD, 2012

Kervalishvili, G. N., and H. Luhr, Climatology of Air Upwelling and Vertical Plasma Flow in the Terrestrial Cusp Region: Seasonal and IMF-Dependent Processes, in *Magnetic Fields in the Solar System, Astrophysics and Space Science Library*, vol. 448, edited by H. Luhr, J. Wicht, S. A. Gilder, and M. Holschneider, pp. 293–329, doi:10.1007/978-3-319-64292-5\_11, 2018.